Automatica 49 (2013) 3562–3570

Contents lists available at ScienceDirect

Automatica

journal homepage: www.elsevier.com/locate/automatica

Point-to-point control near heteroclinic orbits: Plant and controller optimality conditions☆

Brian A. Paden [a,1], Jeff Moehlis [b]

[a] Department of Mechanical Engineering, Engineering II Building, Room 2133, University of California Santa Barbara, Santa Barbara, CA, 93106, United States

[b] Department of Mechanical Engineering, Engineering II Building, Room 2350, University of California Santa Barbara, Santa Barbara, CA 93106, United States

ARTICLE INFO

Article history:
Received 22 March 2013
Received in revised form
5 June 2013
Accepted 8 September 2013
Available online 18 October 2013

Keywords:
Modeling for control optimization
Application of nonlinear analysis and design
Optimization
Optimal control
Heteroclinic orbit

ABSTRACT

In this paper we consider the simultaneous optimization of the controller and plant in a one degree-of-freedom system. In particular we are interested in optimal trajectories between fixed points connected by heteroclinic orbits. We find that designing the plant dynamics to have a heteroclinic connection between target states enables a low energy transfer between the states. We use a nested optimization strategy to find the optimal plant dynamics and control effort for the transition. Additionally, we uncover plant optimality conditions which reduce the complexity of the optimization.

Published by Elsevier Ltd

1. Introduction

The traditional practice for designing mechatronic systems is to first design the structure, sensors, and actuators, followed by the design of the controller. This design approach has been referred to as the sequential or single pass strategy (Fathy, Reyer, Papalambros, & Ulsoy, 2001; Reyer, Fathy, Papalambros, & Ulsoy, 2001; Reyer & Papalambros, 2000). Numerous mathematical and computational tools exist for optimizing these two subsystems independently (Athens & Falb, 1966; Rao, 2009). However, it was proven in Fathy et al. (2001) that this approach does not necessarily satisfy the system level optimality conditions. To solve the problem of finding the optimal plant and controller, several strategies have been proposed. These are classified as iterative, nested, and simultaneous optimization strategies (Fathy et al., 2001). The benefit of these strategies is that they yield an optimal system design, and they have subsequently found their way into a number of engineering applications (Eastep, Khot, & Grandhi, 1987; Grandhi, 1989; Park, 1994; Ravichandran, Wang, & Heppler, 2006).

In this paper, we will consider the energy cost of holding the state of the system at an initial stationary configuration up to an initial time at which the control will transfer the state to a final stationary configuration where it will remain indefinitely. The problem is to choose the best plant dynamics within an admissible design space so that the energy cost associated with the control task is minimized. If it is possible to design the plant so that the initial and final states are connected by a heteroclinic orbit (Guckenheimer & Holmes, 1983) then without external disturbances there will be no cost associated with holding the system at the initial and final states. Then, with little effort from the controller, the plant dynamics will help to carry the state between equilibria in finite time.

This concept is applicable to systems that perform repetitive motion between two stationary configurations, or periodic motion interrupted by periods of motionlessness. This task is common in automated manufacturing and can be applied to save electrical energy costs associated with machine actuation. Alternatively, the ideas presented could be utilized to simultaneously optimize the mechanical design and reference trajectory for a walking robot. Other applications in which this concept has already been applied are in the actuation of electronically controlled engine valves (Parlikar et al., 2005) and for high speed switching of camera filters in satellites (Paden, Chen, & Fiske, 2007). In both of these

☆ The material in this paper was not presented at any conference. This paper was recommended for publication in revised form by Associate Editor Warren E. Dixon under the direction of Editor Andrew R. Teel.

E-mail addresses: bapaden@mit.edu, brian.a.paden@gmail.com (B.A. Paden), moehlis@engineering.ucsb.edu (J. Moehlis).

[1] Tel.: +1 805 451 7739; fax: +1 805 683 9671.

0005-1098/$ – see front matter. Published by Elsevier Ltd
http://dx.doi.org/10.1016/j.automatica.2013.09.030

applications, the plant was designed to introduce favorable system dynamics that reduce the required actuation energy. However, in both cases the plant and controller were designed sequentially with no guarantee of system optimality. The results presented in this paper will provide tools for selecting the optimal plant design from an infinite dimensional space enabling energy savings in these applications.

Throughout this paper we will restrict our attention to plants with conservative dynamics. In mechanical systems where power consumption is a primary consideration, frictional losses are typically designed to be as low as possible. With the use of rolling element bearings and immersion in low viscosity fluids such as air, ohmic losses in an actuator from overcoming friction are often negligible in comparison to overcoming the inertial forces associated with the mass of the mechanical components.

In Section 2 we consider the optimal open loop control to swing around an inverted pendulum to better understand the gains of actuating a system between the fixed points of a heteroclinic orbit. Section 3 extends the problem to finding the optimal plant dynamics as well as the optimal control. For computing the system-wide optimization we will use the nested optimization strategy. An inner loop will optimize the control for each plant design we consider using optimal control theory. The inner loop optimization is covered in Section 4. The outer loop numerically optimizes the plant design by considering the optimal control for each fixed plant design we consider. To reduce the computational expense of this optimization we will derive optimality conditions of the optimal plant design. These conditions are derived in Section 5. In Section 6, a versatile mechatronic system is introduced that we optimize by applying the methods outlined. Conclusions and a discussion of future research are given in Section 7.

2. Heteroclinic orbits and energy efficient motion control

Here we will demonstrate the energy savings associated with introducing plant dynamics favorable to the control task. In particular a heteroclinic orbit connecting the target states is introduced to the plant dynamics. Conceptually, the control will provide a kick that nudges the state away from the unstable fixed point of the heteroclinic orbit. Then a trajectory dominated by plant dynamics transfers the state to a neighborhood of the adjacent unstable fixed point where another kick from the controller nudges the plant onto the unstable fixed point.

We consider a single parameter ω_n as the design variable. In the following section we broaden the set of allowable plant designs to an infinite dimensional space. Consider the problem of finding the minimum energy control torque $u(t)$ to swing around an inverted pendulum of unit mass. The dynamics will be given by

$$\dot{x}_1 = x_2, \qquad \dot{x}_2 = -\omega_n^2 \sin(x_1) + u(t). \tag{1}$$

We want to solve for the minimum energy control effort connecting the initial state, $(x_1(t_0), x_2(t_0)) = (-\pi, 0)$, to the final state, $\big(x_1(t_f), x_2(t_f)\big) = (\pi, 0)$. We consider the state to be in $\mathbb{R}^2$ as opposed to $\mathbb{R} \times S^1$. For $u(t) = 0$ and $\omega_n > 0$ there will be a heteroclinic orbit connecting the target states. We apply Pontryagin's minimum principle (Athens & Falb, 1966) to derive necessary conditions for an optimal control in the form of a boundary value problem (BVP). The cost functional we minimize is

$$J[u] = \int_{t_0}^{t_f} [u(t)]^2 \, \mathrm{d}t. \tag{2}$$

The Hamiltonian for this system and the cost functional is

$$H(x_1, x_2, u, p_1, p_2) = u^2 + \left\langle \begin{pmatrix} p_1 \\ p_2 \end{pmatrix}, \begin{pmatrix} x_2 \\ -\omega_n^2 \sin(x_1) + u \end{pmatrix} \right\rangle, \tag{3}$$

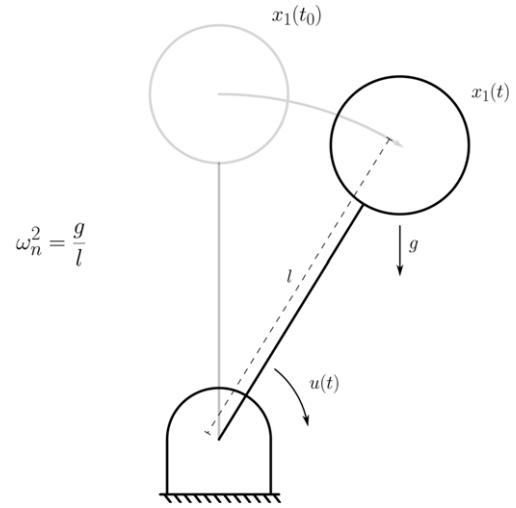

Fig. 1. A simple pendulum with a control torque $u(t)$ swinging the pendulum through a rotation of 2π between unstable equilibria.

where p_1 and p_2 are the co-state variables. Then the canonical equations provide optimality conditions:

$$\begin{aligned} \frac{\partial H}{\partial u} &= 0, \\ \frac{\partial H}{\partial p_1} &= \dot{x}_1, \\ \frac{\partial H}{\partial p_2} &= \dot{x}_2, \\ \frac{\partial H}{\partial x_1} &= -\dot{p}_1, \\ \frac{\partial H}{\partial x_2} &= -\dot{p}_2, \end{aligned} \tag{4}$$

which yield:

$$\begin{aligned} &\dot{x}_1 = x_2, \\ &\dot{x}_2 = -\omega_n^2 \sin(x_1) - p_2/2, \\ &\dot{p}_1 = p_2 \omega_n^2 \cos(x_1), \\ &\dot{p}_2 = -p_1, \\ &u = -p_2/2, \\ &(x_1(t_0), x_2(t_0)) = (-\pi, 0), \\ &\big(x_1(t_f), x_2(t_f)\big) = (\pi, 0). \end{aligned} \tag{5}$$

The case $\omega_n = 0$ is considered as a basis of comparison with various values of ω_n.

The shooting method in conjunction with the Nelder–Mead simplex method (Nelder & Mead, 1965) was implemented to solve (5) for $t_0 = 0$ and $t_f = 10$. ω_n was varied in (5) to demonstrate the benefit of the heteroclinic orbit introduced by the pendulum dynamics. Figs. 1 and 2 illustrate the significant reduction in control effort as ω_n is increased.

3. Problem statement

It is clear that introducing a heteroclinic orbit connecting the target configurations for point to point control reduces the energy cost. With this in mind we now investigate the simultaneous optimization of the plant and control where the set of admissible plant designs is an infinite dimensional space. Specifically we consider a subset of continuous functions on the interval $[x_0, x_f]$.

Consider a system of the form

$$\dot{x}_1 = x_2, \qquad \dot{x}_2 = \alpha f(x_1) + u(t), \tag{6}$$

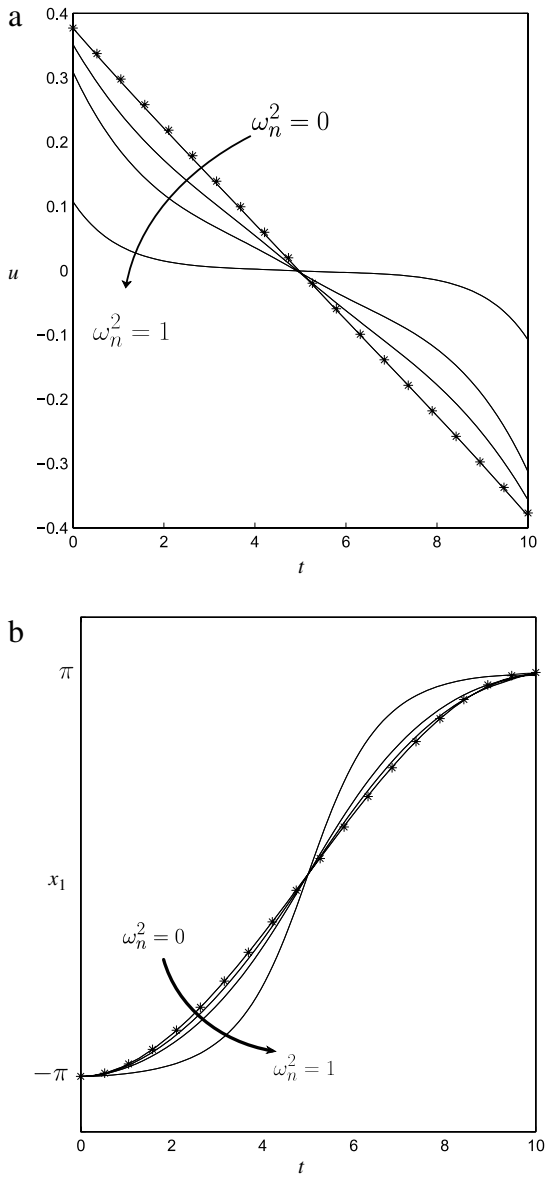

Fig. 2. As ω_n is varied from the values 0, 0.1, 0.3, 0.5, and 1, one can see in (a) the significant reduction in control effort required for the point-to-point control. The effect on the state trajectory can be seen in (b).

with $\alpha > 0$. A trajectory produced under the influence of αf and u will be considered admissible if it satisfies:

$$\begin{aligned}(x_1(t), x_2(t)) &= (x_0, 0) \quad \forall t \in (-\infty, t_0],\\ (x_1(t), x_2(t)) &= (x_f, 0) \quad \forall t \in [t_f, \infty).\end{aligned} \tag{7}$$

That is, up to time t_0 the state is held at $(x_0, 0)$. The control then transfers the state to $(x_f, 0)$, by time t_f. The state must then remain there indefinitely. We will assume without loss of generality that $x_0 < x_f$.

3.1. Conditions of an admissible system design

Here we define the conditions on the control effort, u, and the plant dynamics, f, for an admissible system design. We require that the control effort remain bounded and piecewise continuous; *Ω will denote the set of admissible controls for which these conditions hold.* We require the plant dynamics to satisfy the constraint (8) everywhere on the interval $\left[x_0, x_f\right]$ excluding finitely many points.

$$g(x) \leq \psi(f(x), f'(x), \ldots, f^{(n)}(x)) \leq h(x). \tag{8}$$

It will be required that f be n times piecewise continuously differentiable, and f' be Lipschitz continuous (if n is less than 2 the constraint is satisfied everywhere). The functions g and h are continuous real valued functions defined on $\left[x_0, x_f\right]$. The function ψ is a continuous real valued function from $\mathbb{R}^n$ into $\mathbb{R}$. The functions g, h and ψ, as well as the dimension, n, of ψ are to be determined by the particular application. Assume $g(x) \leq h(x)\ \forall x \in [x_0, x_f]$ so that there may exist an admissible f. For each $x \in [x_0, x_f]$, ψ is evaluated at $(f(x), f'(x), \ldots, f^{(n)}(x))$ and must satisfy (8).

The construction of this constraint captures a broad range of design constraints. However, it does not capture all constraints that could be placed on the plant design space. For example, integral constraints such as a constraint on the L^p norm (for a finite p) of f cannot be expressed in this form. Some examples of constraints that can be expressed in this way are the uniform norm of f or any of its derivatives. We can consider the case when there is no constraint other than Lipschitz continuity of f' by letting $\psi = 0$. These constraints may appear in mechanical systems as limitations on the rate at which f changes in order to control dynamic loads or to satisfy geometric constraints. *We define the set F as the set of all f satisfying (8) with Lipschitz continuous first derivative.*

An ordered pair $(f, u) \in F \times \Omega$ will be referred to as a system design, and a system design will be called admissible if a solution to (6) passing through $(x_0, 0)$ at t_0 is an admissible state trajectory. The cost associated with an admissible system design is

$$J[u, f] = \int_{-\infty}^{\infty} [u(t)]^2 \, \mathrm{d}t. \tag{9}$$

An admissible system design (f^*, u^*) is optimal if $J[u^*, f^*] \leq J[u, f]$ for all admissible system designs. The problem is to find the optimal system design.

3.2. Existence of a control with bounded cost

The existence of a bounded cost control effort when $f(x_0) = 0$ and $f(x_f) = 0$ is easily proven by construction. Choose $x_1(t)$ to be a $C^2[t_0, t_f]$ trajectory satisfying (7). Solving for $u(t)$ in (6) yields

$$u(t) = \ddot{x}_1(t) - f(x_1(t)). \tag{10}$$

It follows from the continuity of f and compactness of $[t_0, t_f]$ that $u(t)$ is bounded on $[t_0, t_f]$. Since $f(x_0) = 0$ and $f(x_f) = 0$, $u(t) = 0$ for $t \notin [t_0, t_f]$. Thus, (9) is bounded.

4. Optimality conditions for the control

Recall that in Section 2 we implemented classical optimal control techniques to compute the minimum energy trajectory between the fixed points of a heteroclinic orbit. Here we will apply the same techniques to (6) to derive the necessary conditions of an optimal u on $[t_0, t_f]$ for a fixed αf in the form of a BVP. This will allow us to find the optimal control for a fixed plant αf. This approach will be used to run the inner loop of the system optimization.

To be clear, we are considering the dynamical system

$$\dot{x}_1 = x_2, \qquad \dot{x}_2 = \alpha f(x_1) + u(t), \tag{11}$$

with $\alpha > 0$ and the cost functional

$$J[u] = \int_{t_0}^{t_f} [u(t)]^2 \, \mathrm{d}t, \tag{12}$$

and boundary conditions

$$\begin{aligned}(x_1(t_0), x_2(t_f)) &= (x_0, 0),\\ (x_1(t_f), x_2(t_f)) &= (x_f, 0).\end{aligned} \tag{13}$$

The Hamiltonian for this system is then

$$H(x_1, x_2, u, p_1, p_2) = u^2 + \left\langle \begin{pmatrix} p_1 \\ p_2 \end{pmatrix}, \begin{pmatrix} x_2 \\ \alpha f(x_1) + u \end{pmatrix} \right\rangle. \tag{14}$$

From (4) we arrive at necessary conditions on an optimal u in the form of a BVP:

$$\begin{aligned} &\dot{x}_1 = x_2, \\ &\dot{x}_2 = \alpha f(x_1) - p_2/2, \\ &\dot{p}_1 = -\alpha p_2 f'(x_1), \\ &\dot{p}_2 = -p_1, \\ &u = -p_2/2, \\ &(x_1(t_0), x_2(t_0)) = (x_0, 0), \\ &\big(x_1(t_f), x_2(t_f)\big) = (x_f, 0). \end{aligned} \tag{15}$$

4.1. Continuous dependence on parameters

It is shown in Oniki (1973) that if there is a unique optimal control at a particular parameter value α_0, then the optimal control and state trajectory are differentiable with respect to α at α_0. Thus, they also depend continuously on α at α_0. Then given $\varepsilon > 0$ there exists α sufficiently close to α_0 such that:

$$\|z(t, \alpha) - z(t, \alpha_0)\| < \varepsilon \quad \forall t \in [t_0, t_f], \tag{16}$$

where $z = (x_1, x_2, p_1, p_2)^T$.

4.2. Properties of the solution to (15) for small α

We now point out an important property of the solution to (15). Let $\alpha = 0$. A unique solution, $\big(\tilde{x}_1, \tilde{x}_2, \tilde{p}_1, \tilde{p}_2\big)$, to the system when $\alpha = 0$ is computed easily since (15) becomes linear. In particular we are interested in $\tilde{x}_2$:

$$\tilde{x}_2(t) = \frac{6(t - t_0)(t_f - t)(x_f - x_0)}{(t_f - t_0)^3}. \tag{17}$$

From (17) we see that $\tilde{x}_2(t) > 0$ on (t_0, t_f). Since, solutions depend continuously on α at $\alpha = 0$. Then for any $\varepsilon > 0$ there exists $|\alpha| > 0$ such that

$$\big|x_2(t) - \tilde{x}_2(t)\big| < \varepsilon \quad \forall t \in [t_0, t_f], \tag{18}$$

where $x_2(t)$ satisfies (15). It follows that for α sufficiently small, $x_2(t) > 0\ \forall t \in (t_0, t_f)$ by the following argument: suppose that there is no such $\alpha > 0$. Then for all $\alpha > 0$, $\exists t^* \in (t_0, t_f)$ such that $x_2(t^*) \leq 0$. From (17), $\tilde{x}_2(t^*) > 0$. Thus, for some $\varepsilon > 0$, $\tilde{x}_2(t^*) - x_2(t^*) = \varepsilon$. This is a contradiction of (16). *For the remaining part of the paper we consider α to be small enough for this property to hold.*

Next, $x_2(t) > 0\ \forall t \in (t_0, t_f)$ and $\dot{x}_1 = x_2$ implies that x_1 is one-to-one on $[t_0, t_f]$. This is also proven by contradiction. Suppose that x_1 is not one-to-one on $\big[t_0, t_f\big]$. Then there are two distinct points τ_1 and τ_2 in $\big[t_0, t_f\big]$ for which $x_1(\tau_1) = x_1(\tau_2)$ (assume without loss of generality that $\tau_1 < \tau_2$). Since x_2 is continuous, x_1 is differentiable. So by application of Rolle's Theorem (Rudin, 1964) there exists a time $\tau^* \in (\tau_1, \tau_2) \subseteq (t_0, t_f)$ where $\dot{x}_1(\tau^*) = 0$, and thus $x_2(\tau^*) = 0$. This is a contradiction of the previous observation that $x_2(t) > 0\ \forall t \in (t_0, t_f)$.

To demonstrate the monotonicity of the x_1 trajectory solving (15), we consider the minimum energy control for (5) with initial conditions $(x_1(t_0), x_2(t_0)) = (0, 0)$ instead of $(x_1(t_0), x_2(t_0)) = (-\pi, 0)$ (i.e. the minimum energy pendulum swing up problem). This problem is solved numerically using the same scheme as in Section 2. By varying ω_n we see that below some critical value, the x_1 trajectory is monotonic. Fig. 3 shows how the minimum energy swing up exhibits oscillations for larger values of ω_n.

The purpose of this example is to demonstrate that the perturbation parameter (ω_n in this case) may be large before the optimal x_1 trajectory loses its monotonicity. Additional numerical experiments suggest that the critical value of the perturbation parameter depends not only on the plant dynamics but also on the transition time and target configurations. For example, in the pendulum swing around problem discussed in Section 2 solving for the optimal control with $\omega_n^2 = 4$ and a transition time $(t_f - t_0) = 5$ yields a monotonic x_1 trajectory while in the swing up problem it does not.

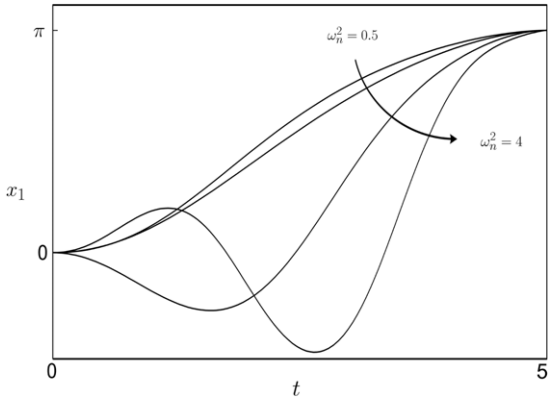

Fig. 3. Minimum energy trajectories for the fixed time pendulum swing up problem. Solutions are computed for ω_n^2 equal to 0.5, 1, 2, and 4.

5. Optimality conditions for the plant

With a procedure to optimize the inner loop (control) of the nested optimization we now consider the optimization of the plant. For each plant design considered we must numerically solve a BVP to find the optimal control effort for that plant design. Thus evaluating the cost of a particular plant design is computationally expensive. For this reason the plant dynamics must be optimized efficiently. Theorem 5 will provide optimality conditions for an optimal plant design. The following lemmas are needed for the proof of Theorem 5.

Lemma 1. *If a pair (f^*, u^*) is optimal, then $f^*(x_0) = 0$ and $f^*(x_f) = 0$; and if no such plant design is admissible, then all designs have unbounded cost.*

Proof. Suppose $f^*(x_0) \neq 0$. (An analogous argument holds for $f^*(x_f) \neq 0$.) Then $u(t) = -f^*(x_0)\ \forall t \in (-\infty, t_0)$ so that the cost (17) is unbounded. This is a contradiction since we have already established the existence of a bounded cost solution when there is an admissible design with $f^*(x_0) = 0$ and $f^*(x_f) = 0$. □

Lemma 2. *Suppose u^* is an optimal control for the system. Then there is no interval $(\tau_1, \tau_2) \subseteq (t_0, t_f)$ where $u^*(t) = 0$ for all $t \in (\tau_1, \tau_2)$.*

Proof. Suppose there exists a time interval (τ_1, τ_2) where $u^*(t) = 0$ for $t \in (\tau_1, \tau_2)$. Then $\dot{u}^*(t) = 0$ for $t \in (\tau_1, \tau_2)$ as well. Since $u^* = -p_2/2$, then $p_2(t) = 0$ and $\dot{p}_2(t) = 0$ for $t \in (\tau_1, \tau_2)$. From (15) it follows that $p_1(t) = 0$ and $\dot{p}_1(t) = 0$ for $t \in (\tau_1, \tau_2)$, the co-states will be zero for all $t > \tau_1$. Then the motion of the system for $t > \tau_1$ is governed by

$$\dot{x}_1 = x_2, \qquad \dot{x}_2 = \alpha f(x_1). \tag{19}$$

From Lemma 1 and (19) the terminal state $(x_f, 0)$ will be a fixed point of the system. Recall that $x_1(t)$ is one-to-one on $[t_0, t_f]$ and $x(t_f) = x_f$. So for $t \in (\tau_1, \tau_2)$, $x_1(t) \neq x_f$. Then $x_1(t)$ cannot reach the fixed point at x_f in finite time. Hence, such a control would lead to an inadmissible trajectory. □

Lemma 3. *If $u \in \Omega$, $\phi \in C^n(t_0, t_f)$ and $\langle u, \varphi \rangle_{L_2[t_0, t_f]} > 0$, then for all $\varepsilon \in \left(\frac{-2\langle u, \phi \rangle}{\|\phi\|^2}, 0\right)$, $\|u + \varepsilon\phi\|_{L_2[t_0, t_f]} < \|u\|_{L_2[t_0, t_f]}$. (If $\langle u, \phi \rangle < 0$ then the statement is instead true for $\varepsilon \in \left(0, \frac{-2\langle u, \phi \rangle}{\|\phi\|^2}\right)$.)*

Proof. For brevity the subscript $L_2[t_0, t_f]$ will be dropped from norms and inner products for the remaining part of this calculation.

$$\begin{aligned}\|u+\varepsilon\phi\|^2 &= \langle u+\varepsilon\phi, u+\varepsilon\phi\rangle \\ &= \langle u,u\rangle + 2\langle u,\varepsilon\phi\rangle + \langle\varepsilon\phi,\varepsilon\phi\rangle \\ &= \|u\|^2 + 2\varepsilon\langle u,\phi\rangle + \varepsilon^2\|\phi\|^2.\end{aligned}$$

Notice that the right hand side of the equation is quadratic in ε. The quadratic equation $0 = 2\varepsilon\langle u,\phi\rangle + \varepsilon^2\|\phi\|^2$ is convex with zeros at $\varepsilon = \frac{-2\langle u,\phi\rangle}{\|\phi\|^2}$ and $\varepsilon = 0$. Without loss of generality, assume that $\langle u,\phi\rangle > 0$. Then $0 > 2\varepsilon\langle u,\phi\rangle + \varepsilon^2\|\phi\|^2$ for all ε greater than $\frac{-2\langle u,\phi\rangle}{\|\phi\|^2}$ and less than 0. Then we conclude that

$$\|u+\varepsilon\phi\|^2 < \|u\|^2 \quad \forall\varepsilon \in \left(\frac{-2\langle u,\phi\rangle}{\|\phi\|^2}, 0\right). \quad \square$$

Definition 4. Define the norm $\|\cdot\|_\dagger$ on $C^n[x_0, x_f]$ by:

$$\|f\|_\dagger \equiv \max\left\{\max\{|f(x)|\},\ldots,\max\left\{\left|f^{(n)}(x)\right|\right\}\right\}$$
$$\forall x \in [x_0, x_f].$$

Theorem 5. *If an optimal design (f^*, u^*) exists, then the constraint (8) is active for all $x \in [x_0, x_f]$ excluding finitely many points.*

Proof. The proof is by contradiction. Suppose that (f^*, u^*) is the optimal design, and that for some $p \in [x_0, x_f]$, (8) is not active. Then by the continuity of ψ there exists a closed interval $[a, b]$ containing the point p such that, $h(x_1) < \psi(f(x_1), f'(x_1), \ldots, f^n(x_1)) < g(x_1)\ \forall x_1 \in [a, b]$. Again, by the continuity of ψ there exists a $\delta > 0$ such that for all $x_1 \in [a, b]$, $h(x_1) < \psi(f(x_1) \pm \varepsilon, f'(x_1) \pm \varepsilon, \ldots, f^n(x_1) \pm \varepsilon) < g(x_1)$ (by $\pm\varepsilon$ we mean the ball in $\mathbb{R}^n$ of radius ε, centered at $\left(f(x_1), f'(x_1), \ldots, f^n(x_1)\right)$ in the uniform norm). Consider any $\phi \in C^n[a, b]$ where $\phi(x) = 0$ for $x_1 \notin (a, b)$. Then for δ satisfying $0 < \delta \le \varepsilon/\|\phi\|_\dagger$, $h(x) < C(f(x_1) \pm \delta\phi(x_1), f'(x_1) \pm \delta\phi'(x_1), \ldots, f^n(x_1) \pm \delta\phi^n(x_1)) < g(x_1)\ \forall x_1 \in [a, b]$.

Now suppose we wanted to maintain the same trajectory as in the optimal design with the plant design perturbed by $\delta\phi$. Then the control effort must be modified to account for the change in the plant design. That is,

$$\begin{aligned}&\alpha f^*(x_1^*(t)) + u^*(t) \\ &\quad = \alpha f^*(x_1^*(t)) + \delta\alpha\phi(x_1^*(t)) + u^*(t) + \eta(t), \\ &\quad \Rightarrow \eta(t) = -\delta\alpha\phi(x_1^*(t)).\end{aligned}$$

Since $x_1(t)$ is one-to-one on $[t_0, t_f]$ it is not difficult to construct ϕ so that $\left\langle u^*(t), \alpha\phi(x_1^*(t))\right\rangle_{L_2(t_0,t_f)} \neq 0$. For example, one could choose ϕ to satisfy $\operatorname{sgn}\left(\phi(x_1^*(t))\right) = \operatorname{sgn}(u^*(t))$ while $x_1(t)$ is on the interval (a, b). Define t_a and t_b by $x_1^*(t_a) = a, x_1^*(t_b) = b$. From Lemma 2 $u(t) \neq 0$ for all t on $[t_a, t_b]$. It then follows from the construction of ϕ and the properties of u that $u^*(t)\phi(x_1^*(t)) > 0$ on $[t_a, t_b]$ which implies $\left\langle u^*(t), \alpha\phi(x_1^*(t))\right\rangle_{L_2(t_0,t_f)} > 0$. Now applying Lemma 3 we know that we can find $\varepsilon \le \delta/\|\phi\|_\dagger$ such that $\|u^* - \varepsilon\alpha\phi\|_{L_2(t_0,t_f)} < \|u^*\|_{L_2(t_0,t_f)}$ and thus, $\|u^* + \eta\|_{L_2(t_0,t_f)} < \|u^*\|_{L_2(t_0,t_f)}$. Then there exists a perturbation from our optimal plant design with a lower cost control. This is a contradiction, and hence the constraints on f must always be active, except possibly at finitely many points. $\square$

It immediately follows from the proof of Theorem 5 and the definition of an optimal system design that if the plant has no constraints other than a Lipschitz continuous first derivative, then an optimal system design does not exist.

The optimality conditions proven in Theorem 5 reduce the computational expense of optimizing the plant design by restricting the optimization to a subset of F. *The subset of the plant design space F where the optimality conditions are satisfied will be denoted $\tilde{F}$.*

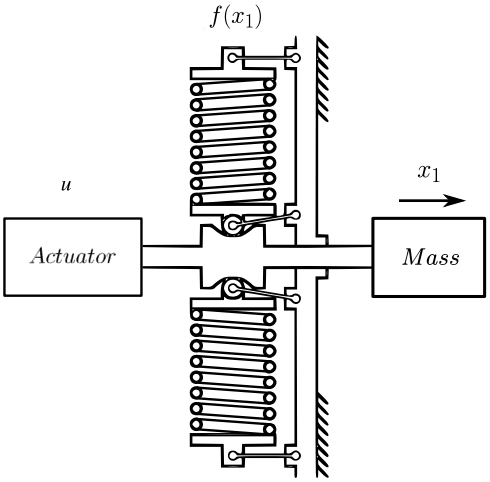

Fig. 4. An actuator provides the control force to the system while the cam assembly provides the desired nonlinear dynamics. The center two pivots allow the cam follower to track the cam profile while the outer pivots are linked together (not shown) so the distance between the two is fixed. This design feature prevents radial loads from being transmitted to the drive shaft as a result of small differences in spring rate of the two springs.

6. Applications to mechatronics

In this section the techniques presented in this paper are applied to the optimization of a simple mechatronic system. The design concept that is shown is intended to provide linear actuation of a mass between two configurations. This mechanism could in practice be a subsystem to a more complex mechanical system. For example in an automated assembly process, an end effector could be modeled by the mass in Fig. 4 which places a component onto an assembly. For simplicity, only linear motion is considered in this example but more complex motion could be engineered while maintaining a single degree-of-freedom.

6.1. Description of the device

Consider the mechatronic system shown in Fig. 4 for linear actuation of a mass between two configurations.

A conventional linear actuator provides a control force directly to the mass through a rigid connection. Coupled in parallel to the actuator is a cam and spring mechanism intended to project a force in the direction of motion that assists the control by appropriate design of the cam. The cam is fixed to the shaft that drives the mass. The cam followers are preloaded against the cam by coil springs and their motion is constrained so that they can only move normal to the motion of the mass. We will assume the cam followers are frictionless and of negligible mass.

6.2. Equations of motion

The displacement x_1 shown in Fig. 4 measures the configuration of the system. The state of the system can be described by the ordered pair (x_1, x_2) where x_1 gives the configuration and x_2 the velocity. It will be assumed that the mass of the payload is much larger than the mass of any other moving parts. The mechanism provides a force $f(x_1)$ on the mass that depends on the configuration. The linear actuator provides the control force $u(t)$ on the mass. The resulting equations of motion are then

$$\dot{x}_1 = x_2, \qquad \dot{x}_2 = f(x_1) + u(t). \tag{20}$$

Now we will calculate how the choice of cam will affect the dynamics and derive the design constraints. Let k be the combined

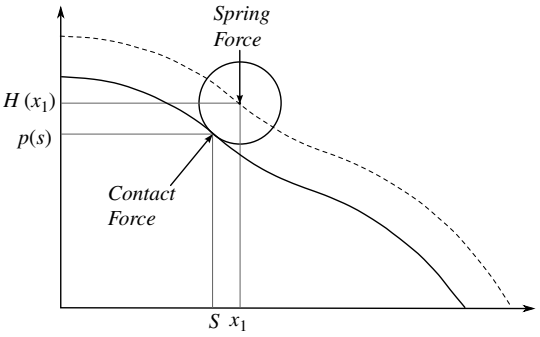

Fig. 5. The cam profile, $p(s)$, and the cam follower path, $H(x_1)$, are distinguished. By varying the contact angle a component of the contact force is projected in the direction of motion x_1.

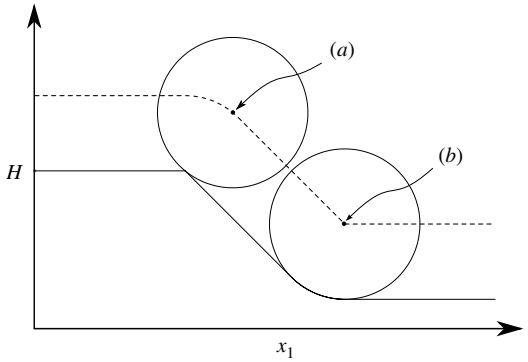

Fig. 6. An illustration of the limitations on the cam follower path's curvature. As the cam follower passes over a corner, it attains its minimum curvature. Alternatively, as the cam profile's curvature becomes equal to the curvature of the cam follower, the curvature of the cam follower's path becomes unbounded.

spring constant of the springs providing force to the cam followers. Let $H(x_1)$ be the displacement of the center of each cam follower away from the rigid shaft with respect to the configuration. Note that the mechanism is symmetric, so each of the cam followers will be of equal distance from the shaft at any particular configuration. Let $H(x_0) = 0$ (recall that x_0 is one of the target configurations described in Section 3). Let r be the radius of the cam follower, and let $p(s)$ describe the cam profile with respect to the contact location s. By examining Fig. 5 it is clear that s is not always equal to x_1. However, it is not difficult to compute $p(s)$ given $H(x_1)$ and vice versa, so it is sufficient to design the mechanism in terms of $H(x_1)$ and compute $p(s)$ for the manufacture of the cams.

We can now compute the force that this setup produces in the direction of motion. A simple calculation yields

$$f(x_1) = k(H(x_1) + \delta_0)H'(x_1), \tag{21}$$

where δ_0 is the deflection of the spring at the initial configuration. We will assume that $\delta_0 \gg H(x_1)$ throughout the interval $[x_0, x_1]$ so that $k(H(x_1) + \delta_0)$ is approximately a constant F_0:

$$f(x_1) = F_0 H'(x_1). \tag{22}$$

The results are unchanged without this assumption, but the calculations become tedious.

Note that the curvature of the cam follower path is given by

$$\kappa(x_1) = H''(x_1) / \left(1 + \left[H'(x_1)\right]^2\right)^{3/2}. \tag{23}$$

In reference to Fig. 6, we see that the minimum curvature of the path taken by the cam follower is $-1/r$ at a corner in the cam profile. The maximum curvature of ∞ takes place as the curvature of the cam equals the curvature of the follower. To control impact and Hertzian contact stress the constraints are modified by adding a tolerance, $\varepsilon > 0$. The constraint on curvature is then

$$-1/(r + \varepsilon) \le \kappa(x_1) \le 1/\varepsilon. \tag{24}$$

We can now express the constraint on the curvature of the cam follower path in terms of the force projected in the direction of motion. Combining (23) and (24), the constraint on curvature in terms of the cam follower path is

$$-\frac{1}{r+\varepsilon} \le \frac{H''(x_1)}{\left(1 + [H'(x_1)]^2\right)^{3/2}} \le \frac{1}{\varepsilon}. \tag{25}$$

Substitution of (22) yields

$$-\frac{F_0}{r+\varepsilon} \le \frac{f'(x_1)}{\left(1 + \left(\frac{f(x_1)}{F_0}\right)^2\right)^{3/2}} \le \frac{F_0}{\varepsilon}. \tag{26}$$

Observe that this constraint takes the form of Eq. (8). Additionally, to apply the results of the previous section to this problem, for $f(x_1)$ satisfying (26) to be an admissible plant design we also require that $f'(x_1)$ be Lipschitz. Without this restriction, $H(x_1)$ could be chosen to have fixed curvature (think of a circular arc). This would be admissible but $f(x_1)$ could grow unbounded on the interval $[x_0, x_f]$. This would lead to unbounded contact stress between the cam surface and cam follower. Requiring Lipschitz continuity eliminates this possibility.

Before moving on to the cam profile optimization it is worth making some remarks on the assumptions made up to this point regarding the mechanism dynamics. We have assumed that the cam follower and coil spring are massless. It is also assumed that there is sufficient preload in the coil spring to achieve constant spring force. In making these assumptions, the calculations are simplified and the possibility of separation between the cam and follower is eliminated. In practice it is necessary to verify the validity of this assumption after designing the follower profile $H(x_1)$ and the trajectory $x_1(t)$. Separation will occur if the contact force between the cam and follower is not greater than zero. A more sophisticated model for the contact force P between the cam and follower projected normal to the x_1 direction is the following:

$$P(t) = m_f \frac{\mathrm{d}^2}{\mathrm{d}t^2}\left(H(x_1(t))\right) + kL \left.\frac{\partial \psi(y,t)}{\partial y}\right|_{y=L}. \tag{27}$$

Here m_f is the follower mass, k is the spring constant, L is the relaxed length of the spring, and $\psi(y, t)$ is the deflection of the spring at each time t and location y along the length of the spring. The mass of the spring m_s is also needed to determine the wave speed of the coil spring when analyzing the spring vibrations. The term $m_f \frac{\mathrm{d}^2}{\mathrm{d}t^2}\left(H(x_1(t))\right)$ is determined directly from the follower profile $H(x_1)$ and the optimal trajectory $x_1(t)$. The term $kL \left.\frac{\partial \psi(y,t)}{\partial y}\right|_{y=L}$ requires solving the partial differential equation

$$\begin{aligned} &\frac{\mathrm{d}^2\psi}{\mathrm{d}t^2} = \left(\frac{L^2 k}{m_s}\right)\frac{\partial^2 \psi}{\partial y^2}, \\ &\psi(0,t) = 0, \\ &\psi(L,t) = \delta_0 + H(x_1(t)), \\ &\psi(y,0) = \frac{\delta_0 y}{L} + H(x_1(0)). \end{aligned} \tag{28}$$

If $P(t)$ becomes negative, then the cam follower will separate from the cam causing undesirable system behavior. Observe that F_0 is an approximation to $k(H(x_1(t)) + \delta_0)$ which is an approximation to $P(t)$. By comparing each of these terms, the assumptions made during the design process can be individually validated.

6.3. Control objective

The control objective is to maintain the state $(x_1, x_2) = (x_0, 0)$ on $(-\infty, t_0)$. Then on $[t_0, t_f]$ the control must transfer the state to $(x_1, x_2) = (x_f, 0)$. The control then holds the system at $(x_f, 0)$ on (t_f, ∞). The goal is to design $f(x_1)$ and $u(t)$ subject to the constraints so that this task is completed while minimizing the energy cost.

6.4. Applying the plant optimality conditions

The following calculation uses Lemma 1 to find a condition on the curvature of the cam follower path:

$$\int_{x_0}^{x_f} \frac{H''(x_1)}{\left(1+[H'(x_1)]^2\right)^{3/2}}\,\mathrm{d}x_1 = \frac{H'(x_f)}{\sqrt{1+\left[H'(x_f)\right]^2}} - \frac{H'(x_0)}{\sqrt{1+[H'(x_0)]^2}}. \tag{29}$$

Making a substitution from (22) we have

$$\int_{x_0}^{x_f} \frac{H''(x_1)}{\left(1+[H'(x_1)]^2\right)^{3/2}}\,\mathrm{d}x_1 = \frac{f(x_f)/F_0}{\sqrt{1+\left[f(x_f)/F_0\right]^2}} - \frac{f(x_0)/F_0}{\sqrt{1+[f(x_0)/F_0]^2}}. \tag{30}$$

Then applying Lemma 1 we have

$$\int_{x_0}^{x_f} \frac{H''(x_1)}{\left(1+H'(x_1)^2\right)^{3/2}}\,\mathrm{d}x_1 = 0. \tag{31}$$

This is a useful constraint to place on the design space.

Next, Theorem 5 with (26) implies

$$\frac{f'(x_1)}{\sqrt{\left(1+\left(\frac{f(x_1)}{F_0}\right)^2\right)^3}} = -\frac{F_0}{r+\varepsilon} \quad \text{or} \quad \forall x \in [x_0, x_f]. \quad \frac{f'(x_1)}{\sqrt{\left(1+\left(\frac{f(x_1)}{F_0}\right)^2\right)^3}} = \frac{F_0}{\varepsilon}. \tag{32}$$

An equivalent way to express this condition is to express it in terms of the curvature of the cam follower path.

$$\kappa(x) = -\frac{1}{r+\varepsilon} \quad \text{or} \quad \kappa(x) = \frac{1}{\varepsilon} \quad \forall x \in [x_0, x_f]. \tag{33}$$

Now since $\kappa(x)$ is limited to two values for this problem, (31) can then be written in the form

$$\int_{x_0}^{x_f} \kappa(x)\,\mathrm{d}x = a\left(\frac{1}{\varepsilon}\right) - b\left(\frac{1}{\varepsilon+r}\right) = 0, \tag{34}$$

where a and b describe the total length in x_1 that have $\kappa(x_1) = 1/\varepsilon$ and $\kappa(x_1) = -\frac{1}{\varepsilon+r}$, respectively. Next we can solve for a and b using

$$a + b = x_f - x_0. \tag{35}$$

Combining (34) and (35) yields

$$a = \varepsilon\frac{(x_f - x_0)}{r+2\varepsilon}, \qquad b = (x_f - x_0) - \varepsilon\frac{(x_f - x_0)}{r+2\varepsilon}. \tag{36}$$

6.5. A hypothesis

We now make the hypothesis that an optimal plant will connect the target states with a heteroclinic orbit, and that the variation in potential energy of the plant across $[x_0, x_f]$ will be maximized. The hypothesis applies specifically to the optimization of this example since in general the constraints on the plant design may not allow for a heteroclinic orbit to connect the initial and the final configuration. This hypothesis is based on the observations in Section 2 that when a heteroclinic orbit was introduced between the target states (via the pendulum potential), the energy cost associated with the point-to-point control decreased. Moreover, the cost continued to decrease as the change in potential energy across $[-\pi, \pi]$ was increased. In the context of this example we will now show that a heteroclinic orbit will connect $(x_0, 0)$ and $(x_f, 0)$ if and only if the following constraints are satisfied:

$$0 = H(x_0) = H(x_f) = H'(x_0) = H'(x_f), \quad H''(x_0) > 0, \qquad H''(x_f) < 0. \tag{37}$$

If $0 = H(x_0) = H(x_f)$ the potential energy of the spring is the same at $(x_0, 0)$ and $(x_f, 0)$, and thus the total energy is the same. Then if $0 = H'(x_0) = H'(x_f)$, $(x_0, 0)$ and $(x_f, 0)$ will be fixed points of equal total energy. Finally, if $H''(x_0) > 0$ and $H''(x_f) < 0$ then $(x_0, 0)$ and $(x_f, 0)$ will be saddle points. Since the plant dynamics conserve the total mechanical energy (without the influence of the control), $(x_0, 0)$ and $(x_f, 0)$ will be connected by a heteroclinic orbit. Conversely, suppose that any one of the conditions in (37) is not satisfied. Then one of the following will occur: at least one target state will not be unstable, or at least one target state will not be an equilibrium of the plant, or the target states will not be on the same level set of the conserved quantity (mechanical energy).

Now consider the follower curvature satisfying the plant optimality conditions and that connects the target states with a heteroclinic orbit:

$$\kappa(x_1) = \begin{cases} -\dfrac{1}{r+\varepsilon} & \forall x_1 \in \left[x_0, \dfrac{x_f - x_0}{2} - \dfrac{\varepsilon(x_f - x_0)}{2(r+2\varepsilon)}\right) \\ \dfrac{1}{\varepsilon} & \forall x_1 \in \left[\dfrac{x_f - x_0}{2} - \dfrac{\varepsilon(x_f - x_0)}{2(r+2\varepsilon)}, \dfrac{x_f - x_0}{2} + \dfrac{\varepsilon(x_f - x_0)}{2(r+2\varepsilon)}\right] \\ -\dfrac{1}{r+\varepsilon} & \forall x_1 \in \left(\dfrac{x_f - x_0}{2} + \dfrac{\varepsilon(x_f - x_0)}{2(r+2\varepsilon)}, x_f\right]. \end{cases}$$

This is the unique plant design satisfying both the optimality conditions and the hypothesis. This is understood most easily by examining Figs. 8 and 9.

Without a proof of the hypotheses, numerical methods are implemented to validate the optimality of the plant design.

6.6. Numerical validation of optimal plant design

When the set $\widetilde{F}$, defined in Section 5, is considered we see that $\kappa(x_1)$ is not necessarily continuous. There can be any finite number of discontinuities in $\kappa(x_1)$ on $[x_0, x_f]$. To numerically validate the optimality of the design in Section 6.5 we will approximate the design space by describing $\kappa(x_1)$ in the following way: $\kappa(x_1)$ will have M square pulses of equal length $\frac{a}{M}$, and there can be no overlap of the square pulses. An example of an admissible curvature of this kind is shown in Fig. 7. The location of each pulse will be described by the design variable y_i. The constraint that the pulses can have no overlap can be expressed as:

$$g_i(y) \equiv y_i - y_{i+1} + \frac{a}{M} \le 0 \quad i = 0, 1, 2, \ldots, M-1. \tag{38}$$

The vector y in (38) is the M-tuple of values y_i. The problem has now been approximated by one that can be analyzed numerically.

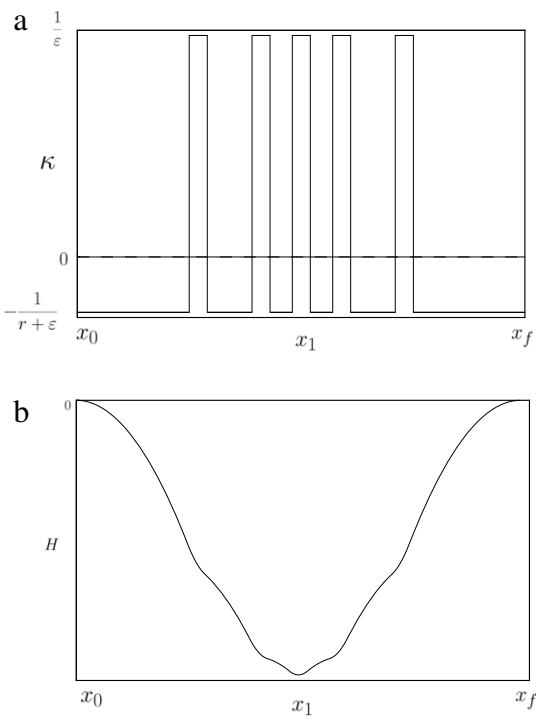

Fig. 7. An example of $\kappa(x)$ in the approximation to the design space where the resulting plant would be admissible and satisfy the necessary conditions given in Lemma 1 and Theorem 5.

Table 1
The numerical values chosen for the optimization problem.

x_0	x_f	t_0	t_f	F_0	ε	r	*Mass*	M
0	1	0	1.5	1	0.1	0.8	1	5

Table 2
Central difference approximation for the gradient of the cost functional evaluated at the candidate solution.

$\frac{\partial J}{\partial y_1}$	$\frac{\partial J}{\partial y_2}$	$\frac{\partial J}{\partial y_3}$	$\frac{\partial J}{\partial y_4}$	$\frac{\partial J}{\partial y_5}$
0.0650	0.0875	0.0350	0.1175	−1.0875

To validate the candidate plant design the following numerical experiment was conducted to check the Karush–Kuhn–Tucker (KKT) condition (Rao, 2009), which is an optimality condition that is frequently used in constrained optimization problems.

6.7. Numerical results

Table 1 shows the values chosen for the numerical experiment. To compute the cost of a candidate plant design the optimal control effort for that particular plant was computed by solving (15) numerically using a shooting method with the Nelder–Mead simplex method to find boundary conditions for the co-state variables. Next the control effort generated by the solution is used to calculate the cost of the design according to the cost functional (9).

In order to check the KKT condition it is necessary to numerically compute the gradient of the cost functional with respect to the parameters of the approximated plant design space. The approach taken is to use a central difference approximation to find the derivative of the cost in the direction of each design variable. For this experiment the dimension of the approximated design space is five. Clearly by the construction of this candidate solution all constraints of (38) are active, so the KKT conditions can

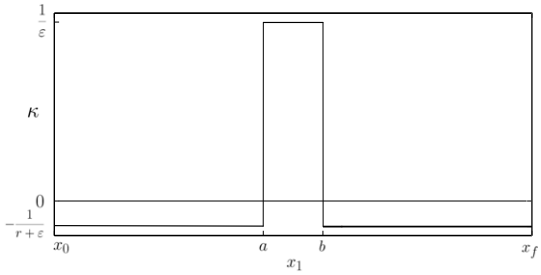

Fig. 8. Plot of optimal cam curvature satisfying the KKT conditions. a indicates the location $x = \frac{x_f - x_0}{2} - \frac{\varepsilon(x_f - x_0)}{2(r+2\varepsilon)}$ and b indicates the location $x = \frac{x_f - x_0}{2} + \frac{\varepsilon(x_f - x_0)}{2(r+2\varepsilon)}$.

be expressed as

$$\frac{\partial J}{\partial y_i} + \sum_{j=1}^{M-1} \lambda_j \frac{\partial g_j}{\partial x_i} = 0 \quad i = 1, 2, \ldots, M, \qquad \lambda_j > 0 \quad j = 1, 2, \ldots, M-1. \tag{39}$$

If we define G as

$$G = \begin{bmatrix} \frac{\partial g_1}{\partial x_1} & \frac{\partial g_2}{\partial x_1} & \cdots & \frac{\partial g_{M-1}}{\partial x_1} \\ \frac{\partial g_1}{\partial x_2} & \frac{\partial g_2}{\partial x_2} & & \\ \vdots & & \ddots & \\ \frac{\partial g_1}{\partial x_M} & & & \frac{\partial g_{M-1}}{\partial x_M} \end{bmatrix}, \tag{40}$$

then (39) can be written as

$$G\lambda = \nabla J. \tag{41}$$

We can then solve for λ:

$$\lambda = \left(G^T G\right)^{-1} G^T \nabla J. \tag{42}$$

Combining the numerical values from Table 2 into (42), the solution for λ is

$$\lambda = [0.2215\ 0.4655\ 0.6570\ 0.9310].$$

Since all values of λ are greater than zero, the KKT conditions are satisfied. The numerical results suggest that the proposed plant design along with a control satisfying (15) will indeed yield the optimal system design. Fig. 8 plots the curvature of this design. The resulting cam, plotted in Fig. 9, illustrates how the constraints described in Fig. 6 are active throughout the cam followers path. It is clear by examining Fig. 9 that the optimal cam design is the one which attains the greatest decrease in spring deflection between the target states while satisfying the optimality conditions. Equivalently, this is the design which maximizes the change from potential to kinetic energy during a switch. Without any influence from the control, the state trajectories would lie on the level sets of the plant Hamiltonian. In Fig. 10 we see how the optimal control gives rise to a trajectory that makes use of the plant dynamics to execute the control objective.

7. Discussion and conclusions

System optimization plays an important role in improving the performance of existing technologies. While the sequential design method can produce satisfactory system performance, it is not guaranteed to yield an optimal system design. In this paper we considered a nested optimization strategy to simultaneously optimize the plant and control, where both were elements of an infinite dimensional space. This presented a computationally expensive optimization even with just a one degree-of-freedom system.

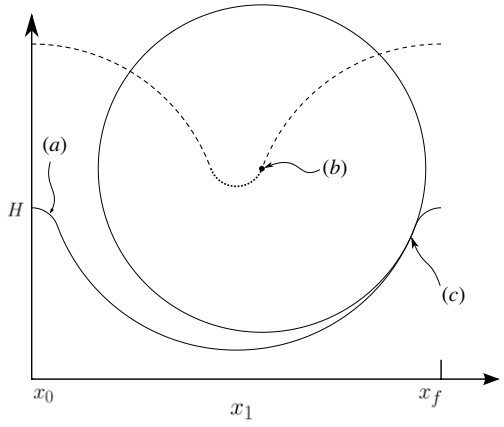

Fig. 9. An illustration of the optimal cam follower path. The dotted and dashed lines show the cam follower path at maximum and minimum curvatures respectively. Arrow (a) indicates the cam profile for the corresponding cam follower path. Arrow (b) indicates the system configuration determined by the center of the cam follower, while arrow (c) indicates the contact location of the cam follower with the cam surface for the illustrated configuration.

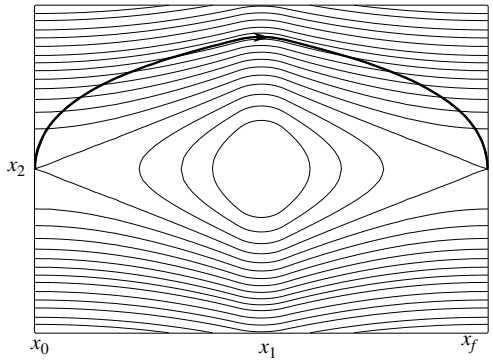

Fig. 10. The optimal state trajectory (in bold) is plotted over the level sets of the Hamiltonian (mechanical energy) of the optimal plant design to demonstrate how the optimal trajectory tends to follow the natural motion of the plant.

The primary result of this paper was to present necessary conditions of an optimal system design to reduce the complexity of the numerical optimization. We began by studying point-to-point control of a plant with pendulum dynamics. It was shown numerically that by increasing the natural frequency, the energy cost of actuating the system between unstable equilibria decreased. This provided the intuition that a mass can be actuated between two configurations with less energy when the two configurations are connected by a heteroclinic orbit.

Then we considered the problem of optimizing the plant and control within infinite dimensional spaces and found that a system optimality condition was that the optimal plant could not lie on the interior of the design space. This result was applied to optimize an electromechanical system with minimal numerical investigation.

There are a number of problems that could be a point of further research. It would be interesting to investigate properties of the critical value for which the optimal trajectory loses its monotonicity. It may be the case that for certain problems, such as ones with heteroclinic orbits connecting target states, that the optimal trajectory is always monotonic and the critical value is unbounded. Another problem that would open the door to additional applications would be to generalize the results to systems with n degrees-of-freedom, and m constraints of the form of (8).

References

Athens, M., & Falb, P. (1966). *Optimal control: an introduction to the theory and its applications*. New York: McGraw-Hill.

Eastep, F., Khot, N., & Grandhi, R. (1987). Improving the active vibrational control of large space structures through structural modifications. *Acta Astronautica*, *15*, 383–389.

Fathy, H. K., Reyer, J. A., Papalambros, P. Y., & Ulsoy, A. G. (2001). On the coupling between the plant and controller optimization problems. In *Proceedings of the american control conference, Vol.3* (pp. 1864–1869). IEEE.

Grandhi, R. V. (1989). Structural and control optimization of space structures. *Computers and Structures*, *31*(2), 139–150.

Guckenheimer, J., & Holmes, P. (1983). *Nonlinear oscillations, dynamical systems, and bifurcations of vector fields, Vol. 42*. New York: Springer-Verlag.

Nelder, J. A., & Mead, R. (1965). A simplex method for function minimization. *The Computer Journal*, *7*(4), 308–313.

Oniki, H. (1973). Comparative dynamics (sensitivity analysis) in optimal control theory. *Journal of Economic Theory*, *6*(3), 265–283.

Paden, B.E., Chen, C., & Fiske, O.J. (2007). Magnetic spring and actuators with multiple equilibrium positions, September 4, 2007. US Patent 7,265,470.

Park, J. H. (1994). Concurrent design optimization of mechanical structure and control for high speed robots. *ASME Transactions on Dynamic Systems, Measurement, and Control*, *116*, 344–356.

Parlikar, T. A., Chang, W. S., Qiu, Y. H., Seeman, M. D., Perreault, D. J., Kassakian, J. G., & Kiem, T. A. (2005). Design and experimental implementation of an electromagnetic engine valve drive. *IEEE Transactions on Mechatronics*, *10*, 482–494.

Rao, S. S. (2009). *Engineering optimization: theory and practice*. New Jersey: John Wiley and Sons.

Ravichandran, T., Wang, D., & Heppler, G. (2006). Simultaneous plant-controller design optimization of a two-link planar manipulator. *Mechatronics*, *16*, 233–242.

Reyer, J.A., Fathy, H.K., Papalambros, P.Y., & Ulsoy, A.G. (2001). Comparison of combined embodiment design and control optimization strategies using optimality conditions. In *ASME design engineering technical conference*. Paper DAC–21119, Pittsburgh, PA, September 2001.

Reyer, J.A., & Papalambros, P.Y. (2000). An investigation into modeling and solution strategies for optimal design and control. In *ASME design engineering technical conferences*. Paper DAC–14253, Baltimore, MD, September 2000.

Rudin, W. (1964). *Principles of mathematical analysis, Vol. 3*. New York: McGraw-Hill.

Brian A. Paden received his B.S. and M.S. degrees at the University of California, Santa Barbara. His research interests are control theory and dynamics. He is currently a doctoral student at the Massachusetts Institute of Technology.

Jeff Moehlis received the B.S. degree in Physics and Mathematics from Iowa State University in 1993, and the Ph.D. degree in Physics from the University of California, Berkeley, in 2000. He was a Postdoctoral Researcher in the Program in Applied and Computational Mathematics at Princeton University from 2000 to 2003. In 2003, he joined the faculty of the Department of Mechanical Engineering at the University of California, Santa Barbara, where he is currently a professor.